



13th IEA Heat Pump Conference  
April 26–29, 2021 Jeju, Korea

## Heat pump and thermal energy storage integration in non-continuous processes – an application to the food industry

Edward J. Lucas<sup>a</sup>, Jan A. Stampfli<sup>a</sup>, Lorenz P. Rast<sup>a</sup>, Raphael Agner<sup>a</sup>, Beat Wellig<sup>a\*</sup>

<sup>a</sup>Lucerne University of Applied Sciences and Arts, Technikumstrasse 21, 6004 Luzern, Switzerland

### Abstract

Industrial sectors routinely represent a considerable share of a country's total energy demand. An increasing emphasis is on heat recovery across the sector and reducing greenhouse gases (GHG). Heat pump (HP) integration offers the potential to realize energy efficiency and GHG reduction, but is often challenging as a significant portion of energy demand is allocated to non-continuous processes. Consequently, heat recovery measures involving thermal energy storage integration are frequently the only option to recover heat indirectly. Additionally, careful consideration of available condensation and evaporation duties using the grand composite curve, and HP operational parameters such as evaporation and condensation temperatures, are required to perform HP integration within the system. A practical procedure for combined heat pump and thermal energy storage (HPTES) integration into non-continuous processes is presented. HPTES parameter selection is addressed using a graphical approach based on pinch analysis. The approach is demonstrated through application to a candy production plant, which produces in three daily shifts of similar duration and procedure. Up to 74.1% utility reduction can be achieved through HPTES integration, with internal rate of return of 11%.

*Keywords:* pinch analysis; heat pump; thermal energy storage; integration; COP curves; non-continuous processes

### 1. Introduction

Industrial sectors across the globe consume a considerable share of total energy demand (EU avg. 24.6%, 2017) [1], and represent a substantial share of total greenhouse gas (GHG) emissions. A large portion of this demand is in the form of thermal energy. Increasingly in industry, emphasis is placed on reducing total energy consumption in order to realize energy and cost savings, and on the consequential reduction of GHGs in accordance with stringent climate-change targets.

Process integration is an established method of accomplishing energy optimization, whereby pinch analysis (PA) is used to determine cost-optimal energy targets for process heat recovery and process hot and cold utility demands [2]. This systematic analysis differentiates processes into two thermodynamically separate subsystems, separated in temperature by a pinch point. Typically, only heating is required above the pinch point and cooling below, allowing a direct calculation of the maximum potential for increasing process energy efficiency.

After exploiting the potential for energy efficiency through direct heat exchange, further savings may be available via indirect heat recovery using thermal energy storage (TES), and heat pump (HP) integration [3]. The latter requires processes still contain considerable amounts of low-grade excess heat and heating demands at suitable temperature levels. Appropriate methods are needed to assess whether HP integration in industrial processes is thermodynamically and economically feasible. Methodologies based on PA have been developed for HP integration using composite curves (CCs) [4], and later grand composite curves (GCCs) [5], which display the deficit heat above the pinch and heat surplus below the pinch [6][7]. While these methodologies were originally constrained to the analysis of continuous process only, later developments of the time slice model (TSM) [8] allowed non-continuous processes to be included in the analysis. Recently, approaches based

\* Corresponding author. Tel.: +41 41 349 37 44  
E-mail address: edward.lucas@hslu.ch.

on the TSM for complete heat pump and thermal energy storage (HPTES) integration using graphical techniques and mathematical programming have been developed [9].

Multiple challenges face HP integration in industry which has prevented widespread adoption of the technology however [10]. Non-continuous processes present particular difficulties when selecting a heat pump with appropriate operational characteristics such as evaporation and condensation temperatures, as well as evaporator and condenser duties for optimal placement across the pinch point [11]. Furthermore, limited expertise and experience represent barriers to entry for the technology and directly affect adoption of the HP technology in industry because of the uncertainty and subsequent financial risks. This is despite such systems being shown to be economically viable, e.g. waste heat recovery from batch reactor systems [12], and a small but growing number of non-continuous process HP integration case studies [13]. Consequently, HP integration has often been relegated to the integration of continuous processes only, restricting the possible contributions of heat pump technology to the reduction in energy consumption across the industrial sector.

This paper aims to reduce these barriers to entry by providing experience and expertise in the form of a case study, helping to support the application of heat pump technology in industry. A procedure based on an optimization approach [9] has been employed to integrate a heat pump into a non-continuous process in the Swiss food and beverage industry.

## 2. Heat pump integration procedure

An overview of the procedure and a concise description is presented here. For brevity, only the most pertinent parts of the procedure are explained to allow readers to understand how the case study data are treated and the results are produced. Only the graphical method of the full hybrid approach has been used here for heat pump integration. A detailed description of the complete hybrid approach including mathematical optimization can be found in Stampfli et al. [9].

### 2.1. Overview of procedure and initial steps

The procedure for integrating a heat pump thermal energy storage (HPTES) system proceeds in 6 steps (Fig. 1). The first step considers the extraction of process data using process control systems, process schematics, and direct measurements where necessary, in order to characterize the process requirements (Step 1). Process scheduling, heating and cooling demands and the economic framework are all required. These

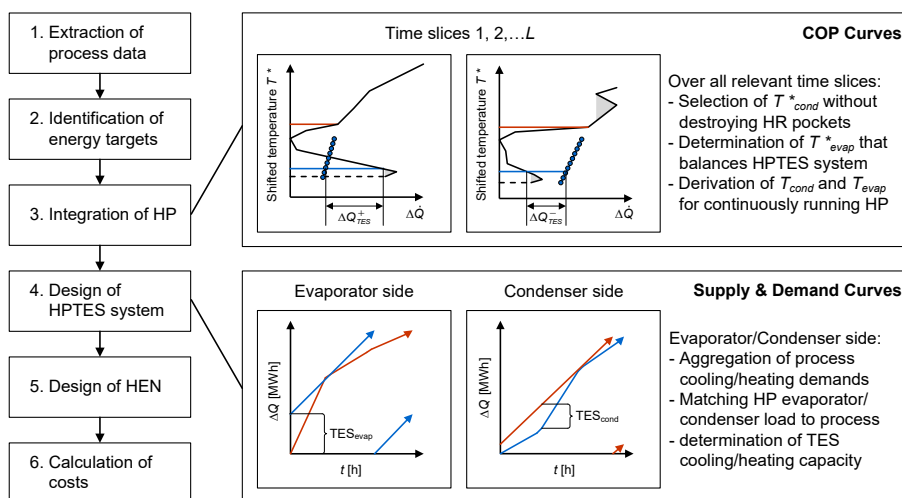


Fig. 1. Procedure for HPTES integration into non-continuous processes

factors form the basis for determination of the energy and cost targets for the process (Step 2) using pinch analysis. Process scheduling directly informs the identification of energy targets through use of the TSM [8].

The process is split into a series of time slices (TSs), according to where the process can be taken as continuous, i.e. periods of time where no streams are beginning or ending in operation, and the available process streams are continuous for the duration of the TS. A change in process heating or cooling requirements dictates the end of the current TS and the beginning of the next. A heat cascade is then calculated for each TS, allowing determination of TS energy targets as well as a pinch temperature during the pinch analysis. When an overall  $\Delta T_{min}$  is selected, a GCC for each TS is produced. The GCC shows the amount of surplus heat below the pinch [6][7], and can be used for HP integration (Step 3). The required condenser and evaporator temperature and maximum duties for each TS are calculated using the GCC and COP curves, as well as the amount of thermal energy that must be covered by the storage system to complete the energy balance across all TSs. This information is used to size the smaller condenser and evaporator duties of the continuously running heat pump that will be integrated using supply and demand curves (Step 4). These curves also allow the calculation of the required storage capacities. Once sizing is completed, a heat exchanger network (HEN) for the system that functions across all TSs can be designed (Step 5). As a final step (Step 6), the costs of the HPTES system are estimated. This includes investment and yearly operational costs, and an estimation of the yearly energy and cost savings.

## 2.2. Heat pump integration using COP curves

The GCCs are used to identify feasible and constant HP evaporation and condensation temperatures despite the varying operational demands of the process. Heat recovery loops (HRLs) incorporating thermal energy storage (TES) are used to cover these variations in the process heating and cooling demands. The storages are often, but not limited to, stratified tanks containing two layers of thermal storage media at near-constant temperature. As the HRL contain HEXs themselves, heat pump evaporation or condenser temperature is shifted from the process stream temperature by several instances of  $\Delta T_{min}$  (Eq. 1).

$$\Delta T = \underbrace{\frac{1}{2}\Delta T_{min} + \frac{1}{2}\Delta T_{min}}_{\text{process stream} \leftrightarrow \text{HRL}} + \underbrace{\frac{1}{2}\Delta T_{min} + \frac{1}{4}\Delta T_{min}}_{\text{HRL} \leftrightarrow \text{HP}} = \frac{7}{4}\Delta T_{min} \quad (1)$$

Between the process streams and the HRL normal heat transfer coefficients are assumed, and therefore two standard temperature contributions of  $1/2 \Delta T_{min}$  are applied [6][7]. For feasible heat transfer between the HRL and the HP, given the high film heat transfer coefficients that occur during phase change of the refrigerant, the temperature contributions are reduced to  $1/2 \Delta T_{min}$  and  $1/4 \Delta T_{min}$ . The resulting temperature differences between process streams and HP is thus a total of  $7/4 \Delta T_{min}$ .

Evaporation and condensation temperatures  $T^*_{evap}$  and  $T^*_{cond}$  determined from the GCC are already shifted with respect to the process streams by  $1/2 \Delta T_{min}$ . The shift from these temperatures to the real temperatures of the evaporator  $T_{evap}$  and condenser  $T_{cond}$  are thus  $5/4 \Delta T_{min}$ :

$$T_{evap} = T^*_{evap} - \frac{5}{4}\Delta T_{min} \quad (2)$$

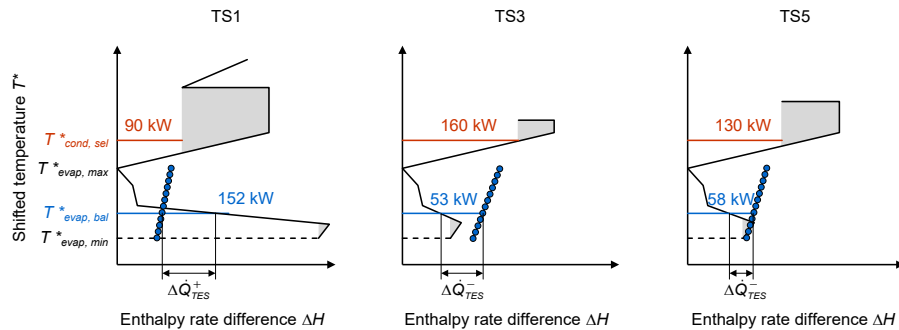


Fig. 2. GCCs of time slices ( $\Delta T_{min} = 5$  K) showing COP curves, taken from case study (transitional period)

$$T_{cond} = T_{cond}^* + \frac{5}{4} \Delta T_{min} \quad (3)$$

The heat pump operating evaporation temperature is found graphically using the COP curves (Fig. 2, blue dots). These curves describe the absorbed heat flow of the HP as a function of the evaporation temperatures and chosen condensation temperature. A condensation temperature  $T_{cond,sel}^*$  is first selected that ensures the heat flow emitted by the HP is maximized (in order to maximize heat recovery) without destroying self-sufficient pockets, and that is as close to the pinch temperature as possible to reduce the temperature lift of the HP and maintain efficiency. An evaporation temperature is then searched between the bounds of  $T_{evap,max}^*$  and  $T_{evap,min}^*$ . An estimation of the amount of heat absorbed is made for each evaporation temperature and plotted on the GCC (blue dots), creating the COP curves. The calculation assumes the HP operates in a reduced-efficiency Carnot cycle with a second-law efficiency of 0.5 (Eq. 4). Usual values for second-law efficiency are around 0.55 [15]. Absorbed heat (evaporation duty) is calculated from the  $COP_{HP}$  (Eq. 5).

$$COP_{HP} = \eta_{2nd\ law, HP} COP_{Carnot} ; \quad COP_{Carnot} = \frac{T_{cond}}{T_{cond} - T_{evap}} \quad (4)$$

$$\dot{Q}_{evap} = \dot{Q}_{cond} \frac{COP_{HP} - 1}{COP_{HP}} \quad (5)$$

Provided the COP curve and GCC intersect, the process cooling demand is exactly equal to the absorbed heat flow by the evaporator. For evaporation temperatures where the absorbed heat is less than the TS cooling demand at this temperature (Fig. 2, TS1), surplus from the process  $\Delta \dot{Q}_{TES}^+$  must be stored in TES. For evaporation temperatures where absorbed heat exceeds the TS cooling demand at this temperature (Fig. 2, TS3&5), heat deficit  $\Delta \dot{Q}_{TES}^-$  has to be provided by storage. The evaporation temperature which satisfies the energy balance of the storage across all time slices  $T_{evap,bal}^*$  is located where the sum of all heat surpluses and deficits across all TSs ( $l = 1 \dots L$ ) is equal to zero, given by:

$$\sum_{l=1}^L \Delta Q_{TES,l}^+ (T_{evap,bal}^*) \cdot \Delta t_l + \sum_{l=1}^L \Delta Q_{TES,l}^- (T_{evap,bal}^*) \cdot \Delta t_l = 0 \quad (6)$$

Where  $\Delta t_l$  represents the TS duration. Once these discontinuous heat flows to and from the TES are known, the TES and HP can be sized using supply & demand curves.

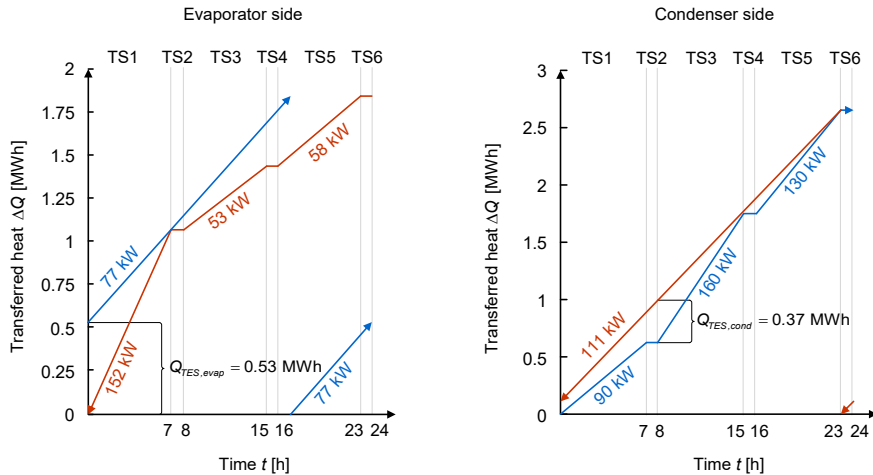


Fig. 3. Supply & demand curves for sizing of HPTES system; values taken from case study

### 2.3. HPTES sizing using supply & demand curves

Supply & demand curves [14] were developed for the sizing of utility systems of non-continuous processes and are used to size the heat pump for continuous operation, as well as size the necessary capacities of the TESs. For the HRL, two such plots exist, one for the evaporator (Fig. 3, left) and one for the condenser (Fig. 3, right). Values are taken directly from the case study data. The diagrams plot the relative flows of heat provided by the HP and demanded by the process across all time slices, which allows calculation of the heat load supplied to or demanded from the TES in order to energetically balance the system.

For the cold HPTES evaporator side, the process TS cooling demands (152 kW, 53 kW, 58 kW) are drawn in red and the HP cooling supply (77 kW) in blue. The maximum discrepancy between the demanded cooling load and the supplied cooling load equals the required TES cooling capacity (0.53 MWh). For the hot HPTES condenser side, process TS heating demands (90 kW, 160 kW, 130 kW) are drawn in blue and the HP heating supply (111 kW) in red. Here, the maximum discrepancy corresponds to the required TES heating capacity (0.37 MWh). It should be noted that during time slices 2, 4, and 6, while no heating or cooling demands are made by the process of the HPTES system, the HP is still in operation. This causes an increase in the heating capacity (hot side) and cooling capacity (cold side) available after these time slices, and hence an increase to the overall required storage capacities on either side of the system.

Without storage, the HP would have to be capable of meeting the process demands directly and would have to be sized according to the maximum demands from the process (evaporator side, 152 kW, condenser side, 160 kW). With TES, the heat pump can run continuously and hence provide the required heat load over a longer duration, reducing the required heat load of the HP.

### 2.4. Heat pump and storage calculations

Storage volume is calculated from the required mass inventories, which are found using the capacities given by the supply & demand curves (0.53 MWh, 0.36 MWh) and the specific heat capacity of the storage media. The inventories must meet the amount of mass needing be transferred during each TS to cover the heating and cooling demand of the streams. A brief summary of pertinent equations is given for the case of the cold HRL i.e. heat transfer to the storage from the hot process streams. For the hot HRL and condenser equations, see [9]. The required mass of storage media in the HRL to cover the heat transfer demands is given by:

$$m_{C,HRL} = \frac{Q_{TES,evap}}{c_{p,HRL}(T_{C,h} - T_{C,c})} \quad (7)$$

Where,  $c_{p,HRL}$  is the specific heat capacity of the media,  $Q_{TES,evap}$  the required cooling capacity, and  $T_{C,h}$  and  $T_{C,c}$  the hot and cold temperature levels of the cold storage.

HP electrical power  $P_{el}$  can then be calculated by completing the energy balance between the emitted heat of the condenser  $\dot{Q}_{cond}$ , the absorbed heat of the evaporator  $\dot{Q}_{evap}$ , and the input power  $P_i$ , assuming a drive efficiency  $\eta_{drive}$  (Eq. 8). An assumption is made that when considering heat pumps of significant size, open type compressors are often used. For open type compressors, where frictional losses to heat are lost to the environment, drive efficiency is assumed to be around 0.9. For closed type compressors, assuming almost all electrical power going into the system is transferred to the refrigerant, this value can be taken as approximately unity ( $\eta_{drive} \approx 1$ ).

$$\dot{Q}_{cond} = \dot{Q}_{evap} + P_i \approx \dot{Q}_{evap} + P_{el}\eta_{drive} \quad (8)$$

## 3. Case Study

### 3.1. Introduction

The case study chosen for analysis is based on a site that manufactures confectionary for the Swiss and European food and beverage markets. To demonstrate more clearly the procedure, the case study data have been simplified, focusing primarily on the parts of the production processes that have substantial heating and cooling demands. The seasonal dependency of certain process streams has been retained, splitting the analysis into three operating cases: Summer (S), Transition Period (TP), and Winter (W). Additionally, the scheduling of the daily production shifts has been modified. The main areas of consideration are:

- Bonbon (BB) Candy Production
- Soft Fruit Candy (SFC) Production
- Hard Fruit Candy (HFC) Production
- Utility Systems

The site produces three types of candy daily, in three consecutive shifts. Although the exact process requirements of each candy variety vary, their manufacture involves the common stages of syrup preparation, mixing, and boiling, as well as casting, drying, and final treatment of the candies. The heating and cooling requirements of these stages are provided for by the on-site utility systems, which consist of hot, warm and cool water circuits. The hot water circuit is heated using steam purchased from off-site, and provides heating to the candy production, the warm water circuit, as well as the domestic hot water and building air handling.

### 3.2. Process description and requirements

In order to proceed with the pinch analysis, the process requirements must be extracted. While the stream data have been adapted for this paper, they originate from stream measurements conducted directly on-site. Process diagrams, monitoring systems and online measurements were consulted to characterize the thermal energy demands of the process. The adapted process requirements are found in Table 1. Where stream identifiers (IDs) have been duplicated between streams, this reflects a sharing of the process equipment between seasons or shifts.

Table 1 Process requirements (AY All Year, S Summer, TP Transition Period, W Winter)

Process Stream	Stream ID	Process period	Inlet T. (°C)	Outlet T. (°C)	CP (kW/K)	Q̇ (kW)	α (W/m²K)
Exhaust Air	H2	AY	55	25	2.43	73	100
Drying Air	C3	S	20	64	2.27	100	50
	C3	TP	12	41	1.92	56	50
	C3	W	5	64	1.27	75	50
BB Vapor 1 bar(a)	H1	AY	99.7	99.6	1200	120	5000
BB Hot Water	C1	AY	95	110	6.0	90	1000
BB Warm Water	C2	S	50	70	20.0	400	1000
	C2	TP	50	70	10.5	210	1000
	C2	W	50	70	13.0	260	1000
BB Cooling Water	H4	S	35	25	28.0	280	1000
	H4	TP	35	25	8.0	80	1000
	H4	W	35	25	6.5	65	1000
BB Cooling	H3	AY	35	25	18.0	180	1000
SFC Vapor 0.5 bar(a)	H1	AY	81.4	81.3	500	50	5000
SFC Warm Water	C2	S	50	70	20.0	400	1000
	C2	TP	50	70	10.5	210	1000
	C2	W	50	70	13.0	260	1000
SFC Cooling Water	H4	S	35	25	17.5	175	1000
	H4	TP	35	25	5.0	50	1000
	H4	W	35	25	3.0	30	1000
HFC Vapor 0.75 bar(a)	H1	AY	91.8	91.7	800	80	5000
HFC Warm Water	C2	S	50	70	20.0	400	1000
	C2	TP	50	70	10.5	210	1000
	C2	W	50	70	13.0	260	1000
HFC Cooling Water	H4	S	35	25	21.0	210	1000
	H4	TP	35	25	6.0	60	1000
	H4	W	35	25	3.5	35	1000

During candy production of any variety, vapor is produced during the boiling and cooking of the gelatin mixtures and according to the temperatures of the cook, the produced vapors vary in pressure (0.5, 0.75, and 1.0 bar absolute). BB production demands the hottest boiling temperatures, and therefore produces the highest vapor pressures. During modelling, all vapor streams are handled as simplified phase changes, having a small temperature difference and a large heat capacity flowrate (CP). After cooking, the candies are formed using cornstarch casts. Before casting can commence the casts must be air-dried, which produces a stream of humid air (Table 1, "Exhaust air"). This humid air is cooled in order to dehumidify it. During dehumidification partial condensation occurs and causes the stream coefficient of heat transfer to increase, as reflected in the table (100 W/m<sup>2</sup>K).

Drying air is also required for candy drying, which takes place immediately after casting. The candies are moved to a drying room where a mixture of fresh air and re-circulated room air is cooled and dehumidified via an adsorption process to maintain the room at a specific temperature and humidity. The fresh air used in this drying process must itself first be cooled and dehumidified, before being sent to the drying room. The candies are left in this room for up to 72 hours at a time, meaning this room is in use throughout the day. Dehumidification processes for building air handling also operate, however only during the summer period. In the final hour of each shift, after the cooking and processing equipment are no longer required, CIP water is used to clean and purge the entire system before the next shift. This cleaning produces wastewater, which is currently used for regenerative heating of the CIP water in a newly constructed heat recovery system. Therefore, the CIP and wastewater were not considered during the integration analysis.

Throughout candy production, warm water and cooling water are both used to provide general heating and cooling, and their requirements vary between seasonal periods. In summer, the dehumidification process for building air is active, and significantly increases both heating and cooling demands compared to winter and the transitional period. In addition to this, warm water demands are higher in winter than the transitional period as a result of lower ambient temperatures. Depending on the variety of candy produced, the cooling water requirements also differ due to differences in the production methods. For BB production an additional hot water stream is used during an intensive cooking phase not required during SFC and HFC production.

### 3.3. Process scheduling

Process scheduling is displayed as a Gantt chart (Fig. 4), which shows the daily production shifts of the plant. Candy production takes place in three shifts, each approximately eight hours in length. This includes an hour for cleaning after production equipment is out of use. The streams associated with heating and cooling during production are assumed continuous over the shift duration, although this is a simplification. Many batches of candies are produced within their 8-hour shift. According to the TSM, the process is divided into six identified Time Slices (TS), although only time slices 1, 3 and 5 are used as the basis for the HP integration. Time slices 2, 4, and 6 were omitted during HP integration as once the wastewater streams were discounted, the exhaust air and drying air streams did not provide enough remaining heat integration for inclusion in the HPTES system according to the pinch analysis.

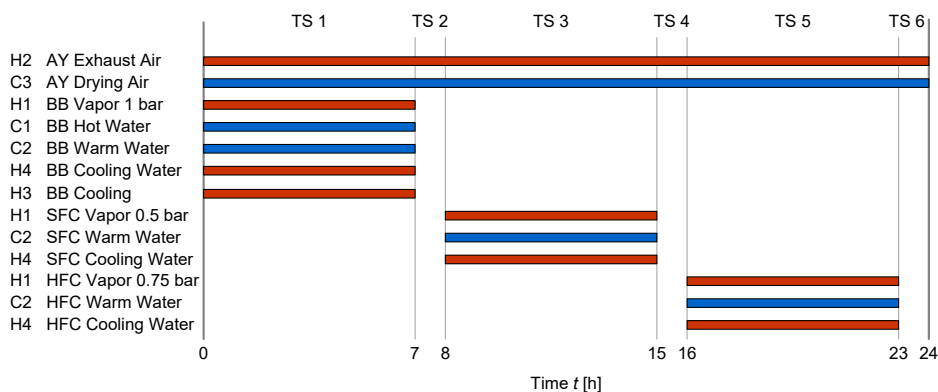


Fig. 4. Gantt-Chart of the daily operating schedule for all seasonal periods

The site is assumed to be in continuous operation 6,000 hours annually. This excludes process downtime such as weekends, in order to simplify the energy targeting analysis [16]. The process hours per individual variety of candy are 438 hours of production and 62 hours of cleaning during summer and winter. During the transitional period, these increase to 875 hours of production and 125 hours of cleaning per candy variety.

### 3.4. Results

#### Heat pump and storage sizing

The heat pump was initially sized using generated time slice GCCs of TS1, TS3, and TS5, displayed in section 2 (Fig. 2). A  $\Delta T_{min}$  of 5 K was selected for all TSs, to avoid the possibility of causing untenably impractical design solutions which require extensive control systems in order to operate successfully. The shown GCCs correspond to the surplus and deficit heat available during the transitional period, which was chosen as a basis for sizing as it is the longest period of seasonal operation. A condensation temperature was selected ( $T_{cond,sel}^* = 67.75^\circ\text{C}$ ,  $T_{cond,sel} = 74.0^\circ\text{C}$ ) that allowed the majority of the required heating demands of all TSs (90 kW, 160 kW, 130 kW) to be satisfied, while remaining as close as possible to the pinch temperature ( $52.5^\circ\text{C}$ ). The COP curves for these time slices were then constructed to locate the initial evaporation temperature. For TS1 there is a relatively large amount of available heat below the pinch point (Fig. 2, TS1), as compared to the later time slices. The heating demands of the process increase from 90 kW in TS1 to 130 kW TS5, peaking at 160 kW during TS3 (Fig. 2, TS3&5). An evaporation temperature was searched ( $T_{evap}^* = 27.6^\circ\text{C}$ ,  $T_{evap} = 21.35^\circ\text{C}$ ) which satisfied the energy balance, resulting in needing TES cooling capacity to cover the cooling demand (152 kW) during TS1, and TES heating capacity to cover the demand for the later time slices (53 kW, 58 kW). These values were then used to construct the supply and demand curves, enabling final sizing of the heat pump condenser (Fig. 3, right, 110 kW) evaporator (Fig. 3, left, 77 kW) as well as the required capacities of the cold and hot side thermal storages (Fig.3, 0.53 MWh, 0.36 MWh). Expressed in cubic meters of water storage, the required storages are  $91.3 \text{ m}^3$  (hot side) and  $60.0 \text{ m}^3$  (cold side). The same approach is used to size the storages and the heat pump for winter and summer operation. However the resulting storage capacities were found to be impractically large requiring in excess of  $200 \text{ m}^3$  of storage, as high energy demands of summer dehumidification processes come online. This amount of storage is only required during summer, and would remain unused during the other seasonal periods which require significantly less energy due to the absence of taxing dehumidification processes. Therefore, it was decided that in order for the system to remain practically viable, the system was sized according to the period of longest duration (transitional period). This still allows significant savings to be realized during summer and winter although does not completely exploit the savings potential inherent therein. Sizing according to the transitional period only provides some additional economic benefit, as storage and heat pump investment costs are relatively reduced and as the system is designed around one continuous operational point, system complexity and control issues are minimized. As a consequence, the full capacity of the storage is in constant use which helps to reduce thermocline degradation.

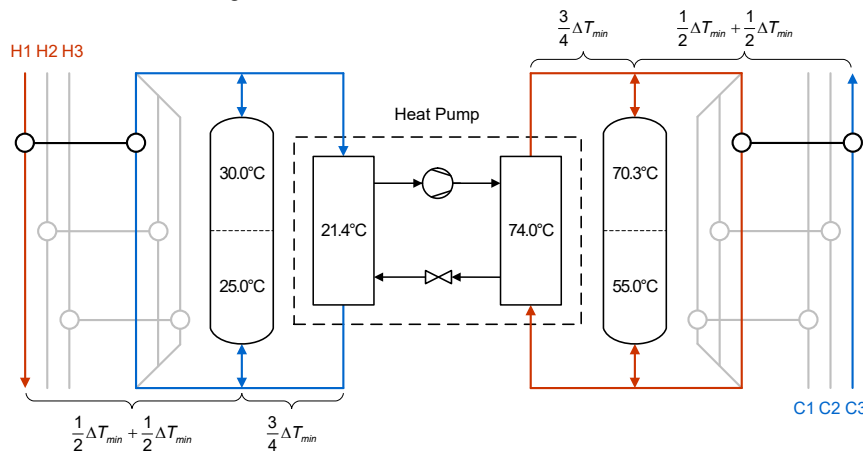


Fig. 5. Conceptual design of the HPTES superstructure



### Design of HPTES system

The conceptual design of the HPTES system is given (Fig. 5) showing the heat pump evaporation and condenser temperatures and the temperatures of the storage layers. A summary of the HPTES specifications appear in Table 3.

Table 3 Heat pump and TES specifications

Pinch T. (°C)	Evaporation /Condenser temperature (°C)	Heat pump COP (-)	Condens er load (kW)	TES Hot storage layer temperatur es (°C)	TES Cold storage layer temperatur es (°C)	TES Hot storage Volume (m <sup>3</sup> )	TES Cold storage Volume (m <sup>3</sup> )
52.5	21.4/74.0	3.3	111	55.0/70.3	25.0/30.0	60.0	91.3

### Design of HEN

The HEN design for the integration of the heat pump and TES system into the process is given (Fig. 6). Integrated streams appear on the right side of the diagram, including the streams HPTES Hot and Cold which represent the intermediate loops of the HPTES system. The design shows the overall HEN with maximum HEX areas, rather than any TS specific HEN where utilized HEX areas may be less than the maximum. HEX areas are displayed beneath their icons. The temperature ranges of the streams are displayed as target and supply temperatures, which begin and end at the pinch ( $T_p = 52.5^\circ\text{C}$ ). The drying air (C3) temperatures are given for each seasonal period (W/TP/S). Utility HEXs have been demarked using arrowed HEXs. The cold utility HEXs have been greyed out, as these are pre-existing heat exchangers which are not considered in the cost calculations. The exhaust air (H2) is a so-called “soft” stream which can provide heating during TSs where this heat can be utilized. If not, the heat is expelled directly to the environment (dotted grey cooler). When calculating energy and cost savings, the cold utility use of this stream is ignored.

### Energy savings of the HPTES integration

The hot and cold utility savings after HPTES integration are tabulated (Table. 6). The utility demands of the process per seasonal period have been summed and are presented alongside the required electrical input to the HP. After HPTES integration, there is a large HU (65.3%) and CU (74.1%) utility reduction, equaling an overall utility reduction of 68.8%. This includes the savings from direct heat recovery measures.

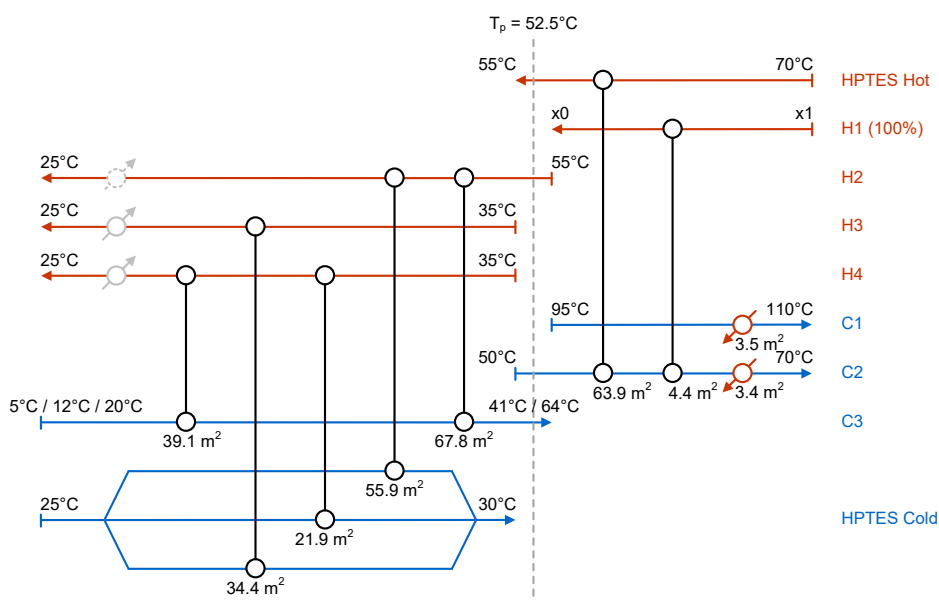


Fig. 6. Conceptual HEN design for candy production (maximum HEX areas)

Table 6 Seasonal energy savings

Seasonal Period	Current state		With HR and HPTES		
	Hot Utility (MWh)	Cold Utility (MWh)	Electrical input (MWh)	HU savings (MWh)	CU savings (MWh)
Summer	651.4	429.1	51.2	283.1	177.9
Transitional Period	651.0	494.5	102.4	568.8	486.2
Winter	436.3	205.1	51.2	284.3	171.9
Total	1,738.7	1,128.7	204.8	1,136.2	836.0

### Financial analysis

The economics of the HPTES system have been analyzed using prices of hot utility (80 CHF/MWh), cold utility (25 CHF/MWh) and electricity (100 CHF/MWh) provided by the industrial partner. A detailing of the finances are found in Table 7. The system requires an investment of CHF 564,000 (including transport, installation, and VAT) which can be paid back within 6.2 years with annual savings of CHF 91,000. The electricity costs of the installation are CHF 21,000. The calculated return on investment for the HPTES and heat recovery system is approximately 11%.

Table 7 Payback and return on investment calculation of heat recovery measures and heat pump integration. Prices include VAT (8%).

Equipment	Investment cost	
HEXs of heat recovery measures (incl. HRL)	CHF	202,000
Heat pump	CHF	147,000
TES	CHF	215,000
<b>Total investment</b>	<b>CHF</b>	<b>564,000</b>
Life time		15 years
Interest rate		3%
<b>Annuity</b>	<b>CHF</b>	<b>47,000</b>
Total savings of heat recovery measures per year	CHF/y	47,000
Total savings of HPTES system per year	CHF/y	44,000
<b>Total savings</b>	<b>CHF/y</b>	<b>91,000</b>
Operational costs of HPTES system per year	CHF/y	21,000
<b>Total operational costs</b>	<b>CHF/y</b>	<b>21,000</b>
<b>Payback</b>		6.2 years
Net income during payback period	CHF/y	23,000
Net income after payback period	CHF/y	70,000
<b>Return on investment</b>		11%

#### 4. Conclusions

A practical procedure for heat pump integration into a non-continuous candy manufacturing process in Switzerland has been presented. The work allows for integration of a continuously running heat pump and thermal energy storage system that can meet daily variations in process demands. The combined heat pump (condenser 111 kW, evaporator 77 kW) and thermal energy storage system achieves an average utility reduction of 68.8% (65.3% cold utility, 74.1% hot utility) and can be paid back within a reasonable economic time frame of 6.2 years., with an internal rate of return of 11% per year. Whilst not a strictly optimal integration, the procedure has provided a practical, workable, and profitable solution for the case study, that is readily understood by the intended end users in industry. As future work it is recommended to apply a complete thermo-economic optimization, using the extended hybrid method which includes mathematical optimization of the HPTES parameters, in order to locate any potential designs which could further increase energy and cost savings without compromising practicability and controllability.

#### Acknowledgements

This research project is financially supported by the Swiss Federal Office of Energy SFOE (contract no. SI/501822-01). It is part of the accompanying research in the Swiss Competence Center for Energy Research SCCER EIP.

#### References

- [1] EU ODP, 2017. European Union Open Data Portal. [online] available from <<https://bit.ly/2NzqQPA>> [Accessed 12 Nov. 2019]
- [2] Linnhoff B., 1993. Pinch Analysis – A state-of-the-art overview. *Trans IChemE* 71, 503–22
- [3] Townsend D.W., Linnhoff B., 1983. Heat and power networks in process design. Heat and power networks in process design. Part I: Criteria for placement of heat engines and heat pumps in process networks, *AIChE J.* 29, 742-748.

- [4] Wallin E., Franck P.Á., Berntsson T., 1990. Heat Pumps in Industrial Processes – an Optimization Methodology, *Heat Recovery Systems & CHP* 10, 437-446
- [5] Wallin E., Berntsson T., 1994. Integration of Heat Pumps in Industrial Processes, *Heat Recovery Systems & CHP* 14, 287-296
- [6] Kemp I.C., 2007. *Pinch analysis and process integration - a user guide on process integration for the efficient use of energy*. 2nd Edition, Oxford, UK, Elsevier Ltd, 25–27
- [7] Smith R., 2016. *Chemical Process Design and Integration*, 2nd Edition, Chichester, UK, John Wiley & Sons, 475-477
- [8] Linnhoff B., Ashton G.J., Obeng E.D.A., 1988. Process integration of batch processes. *ICHEME symposium series*, 109, 221-237.
- [9] Stampfli J.A., Atkins M.J., Olsen D.G., Walmsley M.R.W., Wellig B., 2019. Practical heat pump and storage integration into non-continuous processes: A hybrid approach utilizing insight based and nonlinear programming techniques. *Energy*, 182, 236–253
- [10] Lambauer J., Fahl U., Öhl M., Blesl M., 2008. Large scale industrial heat pump – market analysis, potentials, barriers and best - practice examples, 9th IEA Heat Pump Conference. Zürich, CH
- [11] Olsen D., Abdelouadoud Y., Liem P., Hoffmann S., Wellig B., 2017. Integration of Heat Pumps in Industrial Processes with Pinch Analysis, 12<sup>th</sup> IEA Heat Pump Conference. Rotterdam, NL
- [12] de Boer R., Smeding S., Biesheuvel K., 2017. Waste heat recovery in industrial batch processes: analysis of combined heat storage and heat pump application, 12<sup>th</sup> IEA Heat Pump Conference. Rotterdam, NL
- [13] Schlosser F., Arpagaus C., Walmsley T.G. 2019. Heat Pump Integration by Pinch Analysis for Industrial Applications: A Review. *Chem. Eng. Trans* 76, 7-12
- [14] Wang YP., Smith R. 1995. Time pinch analysis. *Chem Eng Res Des* 73, 905–914.
- [15] Becker HC. 2012. *Methodology and thermo-economic optimization for integration of industrial heat pumps*, PhD Thesis, École Polytechnique Fédérale de Lausanne. Lausanne, CH
- [16] Brunner F., Krummenacher P. 2015. *Einführung in die Prozessintegration mit der Pinch-Methode – Handbuch für die Analyse von kontinuierlichen Prozessen und Batch-Prozessen*, Bundesamt für Energie, CH

## Nomenclature

$c_{p,HRL}$	Heat capacity of storage media [kJ/kgK]	$T^*_{evap}$	Evaporation temperature (shifted) [K]
$l$	Time slices ( $l \in \{1 \dots, L\}$ )	$T^*_{evap,min}$	Minimum evaporation temperature (shifted) [K]
$m_{C,HRL}$	Cold storage media mass [kg]	$T^*_{evap,max}$	Maximum evaporation temperature (shifted) [K]
$\dot{Q}$	Heat flow [kW]	$T^*_{evap,bal}$	Evaporation temperature for energy balance(shifted) [K]
$\dot{Q}_{cond}$	Condenser heat flow [kW]	$T_p$	Pinch temperature [K]
$\dot{Q}_{evap}$	Evaporator heat flow [kW]	$\alpha$	Heat transfer coefficient [W/m <sup>2</sup> K]
$\dot{Q}_{C,HRL}$	Cold storage cooling load [kW]	$\Delta\dot{Q}^-_{TES}$	Heat flow to thermal storage [kW]
$P_{el}$	Heat pump electrical power [kW]	$\Delta\dot{Q}^+_{TES}$	Heat flow from thermal storage [kW]
$P_i$	Heat pump input power [kW]	$\Delta t_l$	Time slice duration [s]
$T_{C,h}$	Cold storage hot temperature [K]	$\Delta T_{min}$	Pinch temperature difference [K]
$T_{C,c}$	Cold storage cold temperature [K]	$\eta_{2nd\ law, HP}$	Second-law efficiency [-]
$T_{cond}$	Condenser temperature [K]	$\eta_{drive}$	Drive efficiency [-]
$T^*_{cond}$	Condenser temperature (shifted) [K]		
$T^*_{cond,sel}$	Selected condensation temperature (shifted) [K]		
$T_{evap}$	Evaporation temperature [K]		

## Abbreviations

AY	All year	GCC	Grand composite curve
BB	Bonbons	GHG	Greenhouse gas
CC	Composite curve	Hx	Hot stream x
CIP	Clean in place	HEN	Heat exchanger network
COP	Coefficient of performance	HEX	Heat exchanger
CP	Heat capacity flowrate	HFC	Hard fruit candy
Cx	Cold stream x	HP	Heat pump
CU	Cold utility		

HPTES	Heat pump thermal energy storage system
HRL	Heat recovery loop
HU	Hot utility
ID	Identifier
IRR	Internal rate of return
PA	Pinch analysis
S	Summer
SFC	Soft fruit candy
TES	Thermal energy storage
TP	Transition period
TS	Time slice
TSM	Time slice model
W	Winter